Cellular and Molecular Biology™ **44** (5), 771-793
Printed in France.

0145-5680/97
1998 Cell. mol. Biol.™

Review

NEW TIME-RESOLVED TECHNIQUES IN TWO-PHOTON MICROSCOPY

Peter T.C. SO[1✍], Karsten KÖNIG[2], Keith BERLAND[3], Chen Y. DONG[1], Todd FRENCH[4], Christof BÜHLER[1], Tim RAGAN[5] and Enrico GRATTON[5]

[1✍] Department of Mechanical Engineering, Massachusetts Institute of Technology, 77 Mass. Avenue, Cambridge, MA 02139, USA
[2] Institute of Anatomy II, University of Jena, Jena, Germany
[3] IBM Research Laboratories, Yorktown, NY, USA
[4] LJL Bio-Systems, Sunnyvale, CA, USA
[5] Laboratory for Fluorescence Dynamics, University of Illinois, Urbana, IL, USA

Received March 22, 1998; Accepted July 15, 1998

***Peter SO**, completed in 1992 his Ph.D. in Princeton University, USA, in the area of morphological phase transition of lipid-water systems. For the next four years, he worked as a postdoctoral research associate in the Laboratory for Fluorescence Dynamics in the University of Illinois, USA, developing fluorescence spectroscopy and microscopy techniques. He is currently an assistant professor at the Department of Mechanical Engineering in the Massachusetts Institute of Technology, Cambridge, USA. His research is focused on the use of multiphoton excitation to study biological processes in systems ranging from single proteins to tissues.*

***Karsten KÖNIG**, studied Physics at the Universities in Rostock and Jena, Germany. He received his Ph.D. on "optical detection of photosensitizers in tissue" in 1989 and his degree as an university lecturer (habilitation) on "optical micro-manupulation and two-photon excitation of living cells" in 1996. His current research in the field of biomedical optics focuses on non-linear effects of laser radiation in cells and tissues.*

***Christof BÜHLER**, received in 1992 his degree in electrical engineering at the Swiss Federation of Technology (ETH) in Zürich, Switzerland. In 1995, he completed his Ph.D Thesis on picosecond spectroscopy of biomolecules. For the following two years, he has been working as a postdoctoral research associate in the field of pump-probe stimulated emission microscopy at the University of Illinois in Urbana-Champaign, USA.*

Abstract - Microscopy is traditionally a tool for determining biological structures. Many recent advances in optical microscopy involves the incorporation of spectroscopy techniques to monitor biochemical states of microscopic structures in living cells and tissues. By minimizing tissue photodamage, two-photon excitation microscopy provides a new opportunity to study the dynamics of biological systems on time scales from nanoseconds to hours. This review will focus on a number of these new methods: two-photon time-lapse microscopy, two-photon photoactivation, two-photon correlated spectroscopy, two-photon single particle tracking and two-photon lifetime microscopy.

Key words: Two-photon, microscopy, time-resolved, photodamage, fluorescence correlation spectroscopy, frequency domain, single particle tracking

INTRODUCTION

Abbreviations: **BSA**: bovine serum albumin; **FCS**: photon correlation spectroscopy; **FFT**: fast Fourier transform; **GPA**: glycogen phosphorylase A; **ROS**: reactive oxygen species; **SPT**: single particle tracking

This renaissance in optical biological microscopy research is partly originated from the improved resolution and sensitivity of modern instruments; significant works include confocal (White *et al.*,

1987), 4-Pi (Hell and Stelzer, 1992; Hell *et al.*, 1994) and standing wave microscopy (Bailey *et al.*, 1993). Another crucial factor driving optical microscopy development is the integration of microscopy imaging with spectroscopy techniques to monitor the interplay between structural and function in living systems. A major obstacle hindering this integration is specimen photodamage which perturbs sample biochemistry and prevents accurate assessment of their functional states. This problem has been significantly alleviated by the recent invention of two-photon microscopy which allows non-invasive monitoring of biological specimen with 3D confocal-like resolution (Denk *et al.*, 1990).

Since two-photon microscopy is still a rather new method for many researchers, we will first provide a brief discussion of this technology. The rest of this review will focus on new combinations two-photon microscopy with time-resolved spectroscopy to monitor biological dynamics. We have taken a broad definition of time-resolved spectroscopy including many techniques that can monitor the temporal evolution of a biological system. The discussion will be structured such that techniques relevant to the dynamics of a particular time scales are grouped. On the time scales of milliseconds and longer, the discussion will focus on time-lapse two-photon microscopy (Wokosin *et al.*, 1996a. 1996b). On the time scale between microseconds and milliseconds, we will discuss two-photon single particle tracking (So *et al.*, 1997), two-photon photo-activation (Denk, 1994) and two-photon fluorescence correlation spectroscopy (Berland *et al.*, 1996). On the time scale between nanoseconds and microseconds, the method of fluorescence lifetime resolved microscopy (So *et al.*, 1995) will be considered.

TWO-PHOTON EXCITATION MICROSCOPY

Maria Göppert-Mayer established the theoretical foundation for two-photon excitation processes in Göttingen, Germany in 1931 (Göpper-Mayer, 1931). The physical principle is the simultaneous absorption of two infrared photons by a chromophore that induces an electronic transition that normally required an ultraviolet photon. The insight that two-photon excitation can be applied to microscopy to obtained high resolution 3D imaging was first conceived by Denk, Webb and coworkers (Denk *et al.*, 1990). Since the two-photon excitation probability is significantly less than the one-photon probability, appreciable two-photon excitation occurs only at a region of high photons flux such as the sub-femtoliter focal volume of a high numerical aperture objective.

In general, two-photon excitation allows 3D biological structures to be imaged with resolution comparable to confocal microscopes but with a number of significant advantages: 1) Conventional confocal techniques obtain 3D resolution by using a detection pinhole to reject out of focal plane fluorescence. In contrast, two-photon excitation achieves a similar effect by limiting the excitation region to a sub-micron volume at the focal point. This capability of limiting the region of excitation instead of the region of detection is critical. Photodamage of the biological specimen is restricted to the focal point. Since out-of-plane chromophores are not excited, they are not subjected to photobleaching. Two-photon excitation ensures economical usage of fluorescent labels. 2) Two-photon excitation wavelengths are typically red-shifted to about twice the one-photon excitation wavelengths. This wide separation between the excitation and emission spectrum ensures that the excitation light and the Raman scattering can be rejected without filtering out any of the fluorescence photons. Furthermore, super-Raman and super-Raleigh scattering have also found to be small (Xu *et al.*, 1997). The improved sensitivity significantly improves the signal to background fluorescence ratio and is critical for studying relatively dim objects. Further, this separation allows the spectroscopic properties across the whole emission spectrum to be monitored. 3) Near-UV chromophores can be excited with near infrared light and imaged without expensive and less efficient UV microscope optics. 4) Two-

photon excitation is more efficient than confocal systems for fluorescence imaging of thick tissue specimens (on the order of 500 to 1000 μm) of large absorption and scattering coefficients. The specimen absorbency in the infrared spectral range is much reduced as compared to the near UV or the blue-green region (Cheong *et al.*, 1990). This minimizes the attenuation of the excitation signal. In addition, for a highly scattering sample, the scattered fluorescence photons are rejected by the detection pinhole and are lost in the confocal case. More fluorescence photons can be collected in the two-photon case with a large area detector and without a pinhole aperture.

Depth discrimination is the most important feature of two-photon microscopy applications. For one-photon excitation in a spatially uniform fluorescent sample, equal fluorescence intensities are contributed from each z-section above and below the focal plane assuming negligible excitation attenuation. This is a consequence of the conservation of energy (Wilson, 1990). On the other hand, in the two-photon case over 80% of the total fluorescence intensity comes from a 1 μm thick region about the focal point for objectives with numerical aperture of 1.25. Thus, 3D images can be constructed as in confocal microscopy, but without confocal pinholes. This depth discrimination effect of the two-photon excitation arises from the quadratic dependence of two-photon fluorescence intensity upon the excitation photon flux which decreases rapidly away from the focal plane. The spatial resolution of two-photon microscopy is comparable to one-photon methods. For excitation of the same chromophore, the two-photon resolution is roughly half the one-photon confocal resolution (Sheppard and Gu, 1990, 1992). This reduction in spatial resolution is due to the larger diffraction limited spot of the longer wavelength two-photon excitation source (double the wavelength of the one-photon source). For a 1.25 N.A. objective using excitation wavelength of 960 nm, the typical point spread function has FWHM of 0.3 μm in the radial direction and 0.9 μm in the axial direction (Figs. 1a, 1b). Two-photon excitation does provide better suppres-

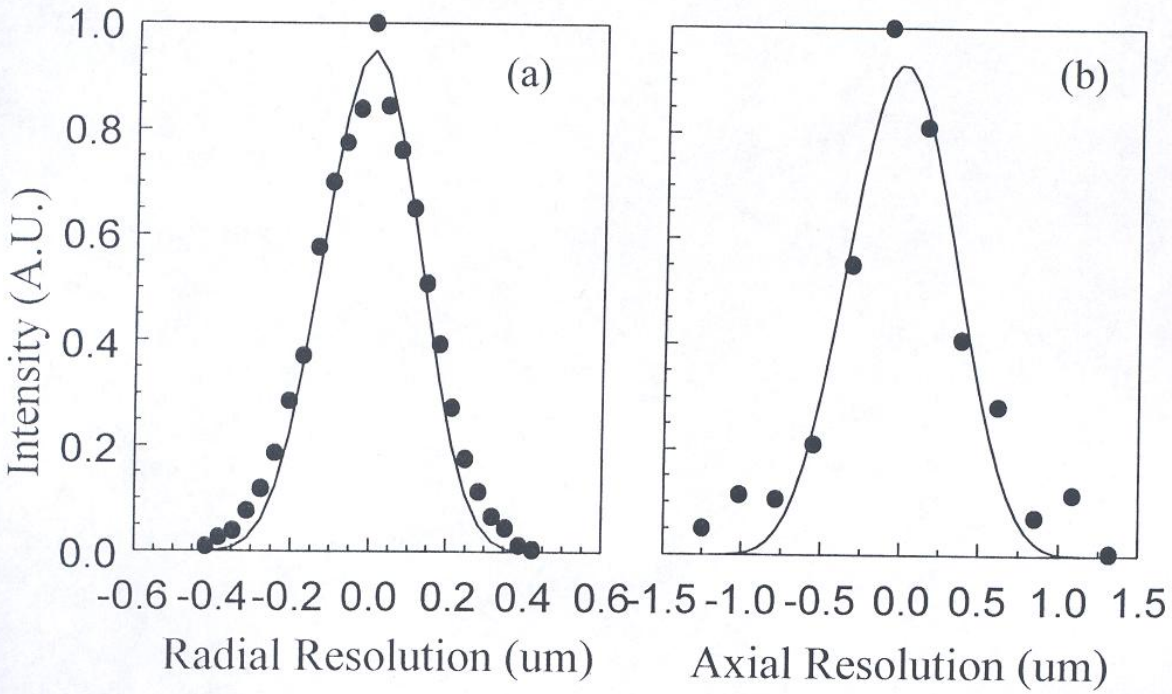

Fig. 1 *Two-photon point spread functions.* Solid line: theoretical prediction. Data points: experimental results obtained from 3D images of 0.03 μm (sub-diffraction limit) fluorescent latex spheres.

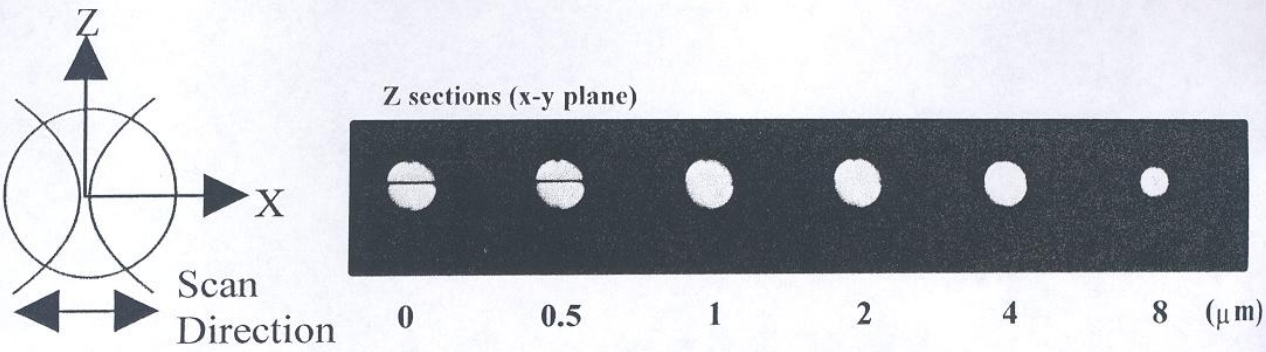

Fig. 2 *Demonstration of the two-photon localization effect.* **a)** The two-photon excitation volume was focused in the center of a 15 μm fluorescent latex sphere. The excitation volume was scanned repeatedly along the x-axis until photobleaching occurred. Afterwards, a 3D image stack of the latex sphere was acquired. **b)** The x-y planes of the sphere at increasing distance from the center are presented. No photobleaching is observed beyond 1 μm.

sion of higher order Airy rings. This localization of two-photon excitation can be best visualized in a simple bleaching experiment (Fig. 2).

TIME SCALES: SECONDS

Two-Photon Time-Lapse Microscopy

– *Significance*: Time-lapse microscopy has been applied to study a large number of biological problems including cell motility (Palecek *et al.*, 1997) and wound healing (Krawczyk, 1971; Stenn and DePalma, 1988). Transmitted light video microscopy is the most common approach in these studies. There are few high resolution, 3D imaging studies of cellular morphological evolution using confocal method. Even more rare is the use of fluorescence confocal microscopy for simultaneous monitoring of cellular biochemistry. The major difficulty involved with fluorescent confocal cellular and tissue imaging is photodamage. There are a number of studies on the effect of high intensity of UV and blue/green radiation on cells and tissues (Cunningham *et al.*, 1985; König *et al.*, 1996a, 1996b). Although the complete mechanism of one-photon photodamage is not well understood, the use of fluorescence confocal for long term monitoring of many biological system is clearly not feasible. Given the need to acquire high resolution structural and biochemical information of the evolution of cellular and tissue structures, an alternative method is needed.

– *Principles*: One of the most critical advantage of two-photon microscopy over confocal method is photodamage reduction. In the simplest case, photodamage can be attributed to the oxidative processes resulting from fluorescence excitation of either cellular endogenous or exogenous chromophore. Assuming uniform chromophore distribution, the degree of photodamage resulting from reactive oxygen species (ROS) generation is correlated with the amount of fluorescence excited inside the cell volume. In the confocal case, fluorescence excitation at each z-section is constant. Therefore, the amount of ROS generated is proportional specimen thickness. In the two-photon case, fluorescence excitation is induced only at the focal point. An equal degree of fluorescence excitation is theoretically needed at the focal region for both the one- and two-photon cases to obtain an equal amount of fluorescence signal. The difference in the amount of ROS generation between the one- and two-photon cases can be approximated by the ratio of the axial dimension of the two-photon excitation volume to the specimen thickness. For typical cellular specimen with a thickness 5 to 10 μm and an excitation volume with axial dimension of 1 μm, ROS generation can be a factor between 5 and 10 higher in the one-photon case. This factor becomes even more significant for thicker specimen such as tissues. Another factors further contribute to the lower photodamage observed using two-photon method is the more efficient detection

light path in a two-photon microscopes which do not need lossy pinhole aperture or de-scanning optics. A practical confocal system will require higher excitation power at the focal volume to obtain the same image quality as a two-photon system. It has been reported that living specimen such as *Ascaris* spermatids can be imaged for at least 60 times longer under two-photon excitation (Wokosin *et al.*, 1996a, 1996b).

– *Application*: The ability to perform long term time-lapse imaging of living specimen has been recognized as a major advantage of two-photon microscopy (Denk *et al.*, 1990). Today, there are large number of successful studies in this area including the study of sea urchine embryos development, the oxygen dynamics of pancreas islet cells, calcium activity in myocytes. Another exciting frontier in this area involves non-invasive imaging of intact organelles (Masters and Thaer, 1994; Piston *et al.*, 1995). Non-invasive study of whole organisms (Masters *et al.*, 1997) may further advance medical diagnostic techniques such as cancer detection and the study of wound healing.

While two-photon excitation is a minimally invasive approach, it is important to recognize that photodamage can still occur at sufficiently high incident power (König *et al.*, 1996a, 1996b, 1997). Time lapse two-photon imaging has also been used to in this area to characterize tissue photodamage mechanisms. Recent experiment has shown that photodamage processes of human sperm is oxidative in nature and is similar to the damage process observed under ultraviolet illumination. Human sperms were placed under two-photon microscope. While it is difficult to subject highly motile sperms to well controlled two-photon irradiation, living sperms that exhibit low motility were chosen for this experiment. Under two-photon illumination with an average power on the order 10 mW, an increase in sperm autofluorescence were first observed in its mid-piece which subsequently intensifies and migrates to the sperm head (Fig. 3). Similar sequence in the alternation of sperm cell autofluroescence is also observed under ultraviolet illumination indicating that two-photon excitation can trigger oxidative damage equivalent to photodamage under ultraviolet illumination.

TIME SCALES: MILLISECONDS AND MICROSECONDS

Two-Photon Photoactivation

– *Significance*: One-photon photoactivation is a powerful technique to observe cellular response to chemical concentration transients on the millisecond time scale. Photolysis of caged compounds such as calcium and neurotransmitters has a wide range of applications. For example, caged calcium has been used extensively in the study of calcium wave (Igarashi *et al.*, 1997; Kirby *et al.*, 1994) and calcium sparks (Niggli and Lederer, 1991; Santana *et al.*, 1997). Two-photon microscopy promises to improve this technique by localizing the photointeraction to within a femtoliter focal volume. This method generates chemical transients that is both confined in time as well as in space. It is important to note that this spatial localization effect cannot be generated with a confocal microscopy which limits the region of observation but not the region of excitation. The study of the local effect of chemical transient such as calcium induced calcium release mechanisms is difficult using traditional photolysis method where the release region of calcium is large and the site where cellular response occur is difficult to localize.

– *Principle*: Many chemical reactions, such as photolysis or polymerization, can be initiated under sufficiently intense illumination. A number of photoliable molecular cages has been developed which photolysis under UV or near UV excitation (Haugland, 1997; McCray and Trentham, 1989). Equivalent to basic two-photon fluorescence excitation, the same photolysis transition can be achieved using infrared photons at a sufficiently high flux. There are two main advantages of using two-photon excitation process to uncage chemical effectors in cells and tissues (Denk, 1994; Denk *et al.*, 1990). First, most common caged compounds

are activated by UV light. The need for high UV power makes cellular damage a major concern. The ability to initiate chemical reaction using infrared light dramatically reduces this problem. Second, the ability to release chemical compounds in a sub-femtoliter volume has enabled novel studies aiming to elucidating the effect of local signaling events. The localization of the reaction volume results from the quadratic dependence of the photolysis probability upon the excitation intensity.

Today, the challenge lies in the low two-photon cross section of typical photoliable cages. Because of this low photolysis cross section, fairly high laser power is needed to release chemical reactants at a sufficient rate to trigger a localized physiological response before Brownian diffusion effectively broaden the interaction volume. The need for high excitation intensity, however, contribute to two problems. First, a high infrared excitation power has been observed to trigger cellular physiological response in the absence of caged compound resulting in a false positive signal (Wokosin *et al.*, 1997). Second, endogenous chromophores, such as NAD(P)H, which is always present in cells, may be preferentially excited and may result in photodamage of the host cells. This may negate the advantage of using infrared instead of UV light in the fist place. Research are currently underway to remedy this difficulty. First, two-photon liable groups with higher efficiency have to be constructed. Considerable success has been attained in developing two-photon fluorescence compound with much higher two-photon absorption coefficient and similar success may be expected in the development of two-photon caged compound (Bhawalkar *et al.*, 1996). Second, most of the currently available photoliable compounds have their absorption maxima at 320 to 340 nm. The wavelength of typical high peak power lasers such as Ti-Sapphire lasers have a minimum operating wavelength of about 690 nm (corresponding to a one-photon wavelength of 345 nm) and cannot effectively activate these probes. Research in developing infrared pulse lasers at this wavelength range is underway.

– *Applications*: Despite these difficulties in two-photon photolysis, a number of innovative studies have been performed. One study focus on mapping ligand-gated ion channels (Denk, 1994). While the function of ligand-gated ion channels have been successfully studied with patch clamp technique, the distribution of these channel in living cells are difficult to determine. In this study, Denk has derived a method to map channel distribution using a combination of two-photon photolysis and whole cell patch clamp technique. Caged carbamoylcholine were dissolved in the bathing medium of BC3H1 cells, a muscle cell line. The two-photon excitation spot was positioned throughout the cell volume to cause a local release of cabamoylcholine. This release will trigger the opening of nicotinic acetylcholine channels which can be detected by monitoring the whole cell ion current using a patch clamp. The current amplitude recorded at each voxel is proportional to the local receptor density. This method has allowed the first

page: 777

Fig. 3 (Top) *A time sequence showing photodamage of human sperm resulted from two-photon microscopy imaging*. The occurrence of photodamage is indicated by an auto-fluorescence increase. This increase was first noted in the mid-piece of the sperm which is then spread to the sperm head within ten seconds. The excitation power on the sperm is about 5 mW and the frame rate of the scan is on the order of two seconds.

Fig. 4 (Center) *Protein dissociation upon dilution as measured by FCS.* **a**) Phosphorylase A (GPA); **b**) malate dehydrogenase (MDH), and **c**) β-phycoerythrin

Fig. 5 (Bottom) *The experimental geometry for macrophage capture of latex spheres*. The yellow arrow indicates the position where the latex sphere was drop. The white arrow indicates the final position of the sphere. The fluorescent plasma membrane of the macrophage has been labelled with Laurdan after the sphere capture experiment. The brightly fluorescent round objects are the captured 2 μm latex spheres. The doted line denotes the outline of the macrophage.

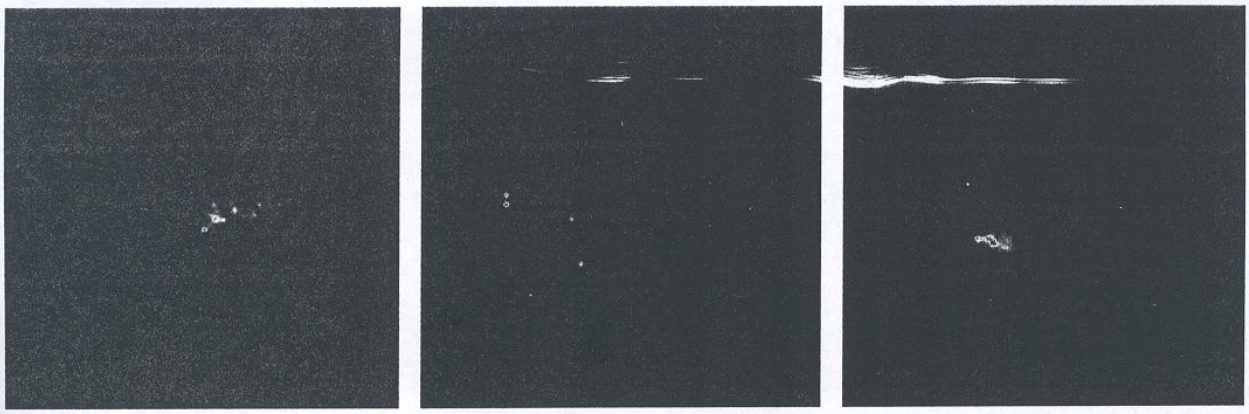

3


0
100
(A.U.)

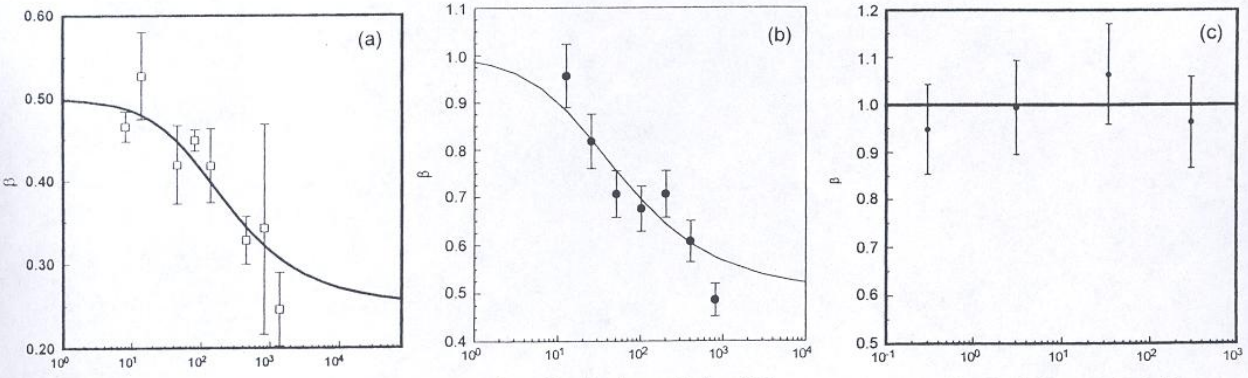
(a)
(b)
(c)
β
Total Protein Concentration (nM)
Total Protein Concentration (nM)
Total Protein Concentration (nM)

4

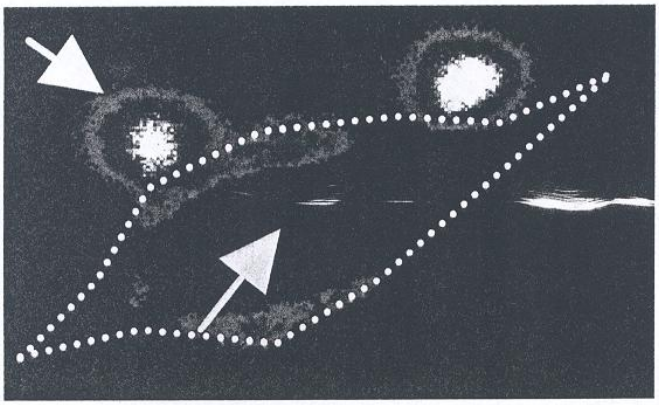

5

high resolution mapping of acetylcholine receptor distribution in living cells. Another promising study involve the two-photon photolysis of caged calcium (Lipp *et al.*, 1997). These authors have obtained a promising preliminary result in studying calcium dynamics in Hypocampus neurons. By permeating the cell with 1 mM of either DM-nitrophen or NP-EGTA, two-photon uncaging of calcium confined spatially to within 1-20 μm has been accomplished with 10-100 mW laser power.

Photon Correlation Spectroscopy

– *Significance*: Fluorescence correlation spectroscopy (FCS) was developed by Elson and Webb in the early 1970s (Elson and Webb, 1974; Elson *et al.*, 1974) to monitor kinetic events in biological system on the time scale from microsecond to milliseconds. However, there are few applications of this technique in the past twenty years. Since the FCS signal amplitude is inversely proportional to the number of fluorescent particles in the observation volume, high sensitivity FCS measurement is difficult in bulk solutions or cellular systems with large number of particles. The majority of the earlier biological FCS studies focus only on membrane systems where the relevant volume is two dimensional and is inherently small (Fahey and Webb. 1978; Meyer and Schindler, 1988). The recent introduction of confocal and two-photon excitation techniques has reduced the observation volume to femtoliters and has opened up many new opportunities in biology. Today, FCS has been applied to the study of receptor binding (Rauer *et al.*, 1996), protein polymerization (Berland *et al.*, 1996), chromophore triplet state transitions (Widengren *et al.*, 1995), ultra-sensitive DNA hybridization assay (Kinjo and Rigler, 1995; Oehlenschlager *et al.*, 1996) and cytosol viscosity (Berland *et al.*, 1995) measurements. The use of two-photon excitation has significantly broadened the applicability of FCS in biological systems (Berland *et al.*, 1995, 1996). Compared with other conventional fluorescence diagnostic methods, FCS offer three important advantages. First, FCS is extremely sensitive. With an optimized optical system, detection at the single molecule level can be routinely achieved (Mertz *et al.*, 1995). While most fluorescence techniques work with sample concentration in the range between nM and μM, FCS extends fluorescence spectroscopy to the sub-nanomolar concentration levels. Second, FCS is a precise and quantitative method. As an example, one of the most common biochemical applications of fluorescence spectroscopy is the monitoring of molecular association and binding by polarization. Fluorescence polarization detects binding events by measuring a change in the rotational diffusion rate of the molecule. However, the quantitative interpretation of the polarization data requires a knowledge of many additional parameters such as molecular shape, dipole orientation and quenching and energy transfer mechanisms. In contrast, FCS measures changes in the molecular translational diffusion coefficient which is a robust parameter with minimal sensitivity to external factors. More importantly, the solution particle density distribution can be directly measured by FCS in combination with high order analysis (Palmer and Thompson, 1987, 1989). Third, the kinetic properties of biological systems can be measured by FCS under equilibrium conditions without external perturbations required for techniques such as fluorescence photobleaching recovery (Luby-Phelps *et al.*, 1986).

– *Principles*: The basic physics underlying this technique can be understood qualitatively. FCS measures the intensity fluctuation of fluorescent molecules. Depend on the mechanism causing these intensity fluctuation, the fluctuation amplitude may contain physical information such as the particle number density, diffusion coefficient, flow rate or their conformations. Consider the most common situation where the intensity fluctuation is caused by Brownian diffusion of molecules into and out of the sample volume. The intensity fluctuation contains information about the particle number density and the diffusion rate. A knowledge of the molecular number density allows the determination of the degree of molecular aggregation. A knowledge of the diffusion rate allow the hydrodynamic radius of the molecule to be inferred.

Consider a sample volume containing n particles. The number of particles in this volume as a function of time is governed by Poisson statistics. The number of particle inside this volume will fluctuate in time with a magnitude equal to $\sqrt{n}$ and the fractional amplitude of the fluctuation is $\frac{1}{\sqrt{n}}$. Thus, for a volume containing one particle, the fractional fluctuation would be 100%; for a volume containing one million particles, the fractional fluctuation would be only 0.1%. The number density of the particles can be determined by experimentally measuring the ratio between the signal amplitude and its fluctuation level. The number fluctuation duration further contains information of the particle diffusion rate. The duration of these fluctuations is related to the time for the particle to transit the observation volume. The diffusion rate of these particles can be calculated from the average fluctuation duration given the size of the observation volume.

The previous description of the FCS principle can be formulated mathematically. The time dependent intensity fluctuation is quantified by the auto-correlation function, G(τ), which is defined as:

$$G(\tau) = \frac{< \delta F(t)\delta F(t+\tau) >}{< F^2 >} \quad (1)$$

where $\delta F(t) = F(t) - < F >$ is the fluorescence intensity fluctuation. F(t) is the fluorescence detected at time t. τ is the time separation between two intensity measurements. The angular bracket represents a time average. The fluorescence intensity fluctuation is proportional to the fluorophore concentration fluctuation scaled by the laser excitation intensity. For two-photon excitation:

$$\delta F(t) = \int d^3\vec{r}\,\delta F(\vec{r},t) = \alpha \int d^3\vec{r} I^2(\vec{r})\delta C(\vec{r},t) \quad (2)$$

$\delta F(\vec{r},t)$ is the fluorescence fluctuation per unit volume at position $\vec{r}$ and time t. α is a product of the excitation cross section, the fluorescence quantum efficiency and the detection efficiency. $I(\vec{r})$ is the excitation photon density per unit volume at position $\vec{r}$. The quadratic dependence on excitation photon intensity is a result of two-photon excitation. $\delta C(\vec{r},t)$ is the fluorophore concentration fluctuation.

Considering the simplest case where the intensity fluctuation is caused by Brownian diffusion driven number fluctuation, the time evolution of the particle concentration can be evaluated. The time evolution of the fluorophore concentration is described by the diffusion eq.:

$$\frac{\partial \delta C(\vec{r},t)}{\partial t} = D\nabla^2 \delta C(\vec{r},t) \quad (3)$$

where D is the diffusion coefficient. For the diffusion of molecules with radius R in a solution of viscosity η, the diffusion coefficient can be estimated from the Stokes-Einstein eq.:

$$D = \frac{kT}{6\pi\eta R} \quad (4)$$

where kT is the Boltzmann temperature factor. For three dimensional diffusion, this differential eq. can be solved:

$$< \delta C(r,t)\delta C(r,t+\tau) >=< C > (4\pi D\tau)^{-\frac{3}{2}} \exp\left(\frac{-|\vec{r}-\vec{r}'|^2}{4D\tau}\right) \quad (5)$$

The autocorrelation function becomes:

$$< \delta F(t)\delta F(t+\tau) >= \alpha^2 \int d^3r \int d^3r' I^2(r) I^2(r') < C > (4\pi D\tau)^{-\frac{3}{2}} \exp\left(\frac{-|\vec{r}-\vec{r}'|^2}{4D\tau}\right) \quad (6)$$

Using Lorentzian-Gaussian intensity distribution approximation, this function can be simplified:

$$< \delta F(t)\delta F(t+\tau) >= \frac{2\alpha^2 I_0^4 w_0^6}{\lambda^2 (4\pi D\tau)^{\frac{1}{2}}} < C > g(D,\tau) \tag{7}$$

where

$$g(D,\tau) = \int db \frac{\exp(-\frac{z_R^2 b^2}{2D\tau})}{b^4 + (2+\frac{16D\tau}{w_0^2})b^2 + \frac{1}{4}(\frac{16D\tau}{w_0^2})} \left[\frac{2b^2 + \frac{16D\tau}{w_0^2} - 4}{\sqrt{2}(2+b^2)} + \frac{2}{\sqrt{2+b^2+\frac{16D\tau}{w_0^2}}} \right]$$

This last integral has no closed form and has to be evaluated numerically.

Note that in the limit of τ approaches zero, one of the 3D spatial integrals in eq. 7 reduces to a product of a three dimensional delta function and <C>, the average particle concentration. Substituting this result into eq. 1, we obtain:

$$G(0) \propto \frac{1}{< C >} \propto \frac{1}{N} \tag{8}$$

where N is the number of particles in the volume. The eq. indicates that the magnitude of the fractional fluctuation is inversely proportional to the number density of the particles substantiating the result that we have derived qualitatively in the previous section. Further note that the eq. 7 is a function of the diffusion coefficient that can be deduced from the functional form of the measured auto-correlation function.

– *Applications*: Two-photon fluorescence correlation spectroscopy is well suited to a number of biological studies. Intracellular diffusion rate in the cytoplasm has been determined using this approach (Berland *et al.*, 1995). Fluorescence latex spheres of 7 nm radius has been introduced into the cytoplasm of mouse fibroblast cells by electroporation. Two-photon fluorescence correlation spectroscopy indicates that the diffusion rate of this spheres were reduced by a factor of ten in the presence of the cytoplasmic matrix as compared to water. The diffusion rate further decreased by another factor of ten within the next hour. The reason for the further slow down remains to be investigated. Plausible explanations include the aggregation of intracellular proteins to the spheres or the active segregation of the spheres by the cell.

Another application involves the use of two-photon correlation spectroscopy to monitor concentration driven oligomerization of protein in bulk solution (Berland *et al.*, 1996). As a result of the quantitative nature of this technique, the exact number concentration of the proteins can be determined. The dissociation of glycogen phosphorylase A (GPA) (Fig. 4a), malate dehydrogenase (MDH) (Fig. 4b) and β-phycoerythrin (Fig. 4c) upon dilution has been monitored. GPA is known to be a tetramer at micromolar or higher concentrations and dissociates to a dimer. MDH is know to dissociate from a dimer to monomers. β-phycoerythrin does not dissociate over the experimental concentration range. The dissociation constants of GPA and MDH are measured to be 430 nM and 144 nM respectively which is in reasonable agreement with previously published results (Huang and Graves, 1970; Ruan and Weber, 1993; Shore Chakrabarti, 1976).

Two-Photon Single Particle Tracking (SPT)

– *Significance*: Three-dimensional transport mechanisms on the time scale of milliseconds are crucial in many areas of cellular biology inclu-

ding membrane receptor internalization and turnover (Deurs *et al.*, 1989; Schwartz, 1990; Watts and Marsh, 1992), organelle transport during mitosis (Salmeen *et al.*, 1985), phagocytosis of antigenic material (Cohen *et al.*, 1994; Maniak *et al.*, 1995), and nucleo-cytoplasmic trafficking of synthesized protein and nucleic acid (Dingwall and Laskey, 1992). In medicine, virus-membrane docking and the subsequent transfer of genetic material (Oneill *et al.*, 1995), endocytosis of protein toxin (Sandvig *et al.*, 1992), and the invasion of intracellular bacterial pathogens (Morisaki *et al.*, 1995; Oh and Staubinger, 1996) are major areas where an understanding of 3D transport mechanisms would play a key role in disease prevention and treatment. Trafficking inside a complex three dimensional environment is a shared common theme. These trafficking processes are rarely passive or diffusion-controlled in cellular systems but are guided by active mechanisms including molecular motors and ion pumps (Goldstein *et al.*, 1985; Rothman, 1994).

Despite our general understanding of these transport pathways, there are many important details of the transport mechanism missing. The difficulties associated with understanding these fundamental processes are twofold. First, many of these motions are directed and under the active control of cellular mechanisms. These complex sequences of events are difficult to resolve when the action of many cells are asynchronously averaged. Second, many of these process are fast, on the order of milliseconds to seconds. Inherently static techniques such as electron microscopy cannot study these fast phenomena. There is a need for an alternative technology that can follow individual particles transported in three dimensions.

Single particle tracking (SPT) was first developed in the early 1980s to address this problem (Ghosh and Webb, 1988, 1994). SPT has four unique features: 1) SPT maps the entire itinerary of each particle under transport. Each step of the transport process can be analyzed. This information is impossible to obtain from the average behavior of many "asynchronized" particles. 2) SPT has excellent time resolution. Current SPT apparatus have achieved a resolution of 33 ms. 3) SPT has excellent spatial resolution. Particles can be located with a precision of tens of nanometers, which is needed to distinguish between diffusive and directed processes. 4) SPT works with biological systems *in vivo* and permits the biochemical environment in the vicinity of the transported particle to be studied with sub-millisecond resolution. This is crucial in delineating the biochemical mechanism which drives the transport.

The first SPT study followed the diffusion of membrane bound low density lipoprotein receptors in two dimensions (Ghosh and Webb, 1994). This approach utilized high sensitivity fluorescent imaging with a video rate intensified CCD camera under wide field illumination. Before the invention of this technique, one could only measure the average transport properties of these receptors as characterized by their membrane diffusion coefficient using techniques such as photobleaching recovery. Using single particle tracking, non-equilibrium transport kinetic behavior has been observed; single receptors are shown to exhibit diffusive, restricted as well as directed motions (Ghosh and Webb, 1994; Jacobson *et al.*, 1994; Saxton, 1994). The development of this technology has opened a new line of inquiry into the dynamics of membrane bound proteins. With few exceptions, most recent applications focus on measuring membrane protein interactions including studies of integrin-cytoskeletal interaction (Schmidt *et al.*, 1994), diffusion of concanavalin A and Thy1 molecules in the plasma membrane (Hicks and Angelides, 1995; Sheetz *et al.*, 1989) and lipid diffusion on a bilayer surface (Fein *et al.*, 1993). The scope of these studies is partially dictated by the two dimensional nature of the instrumentation.

As discussed previously, there are many important studies of biological processes which would benefit from particle tracking in three dimensions. The potential of using particle tracking in three dimensions was first realized by Kao and Verkman

(1994). A cylindrical lens element was added to the excitation beam path to encoded a difference in the aberration pattern for a particle above and below the focal plane. Through a de-convolution routine during data analysis, they can recover the particle's trajectory in three dimensions. This technique has been successfully applied in the study of water permeability of Chinese hamster ovary cells. Although this technique constitutes a first step in developing a 3D tracking technique, it has two major drawbacks that emphasize the need for an alternative technology. First, the axial tracking range of the instrument remains limited to 5 μm. At longer distances, tracking has to be interrupted and the stage repositioned. Moreover, the axial positioning sensitivity is not constant over the entire tracking range but degrades at its limit. Second, the time resolution of this instrument is limited to video rate and cannot study many faster processes.

– *Principles*: A new 3D particle tracking strategy has been developed based upon two-photon excitation circumventing the past difficulties. Since two-photon excitation is inherently a 3D technique with sub-femtoliter volume resolution, the localize the slow moving particles in three dimension is relative straight forward. However, since standard two-photon imaging is inherently a sequential technique and is much slower than CCD imaging which is a parallel acquisition method, the time required to gather a 3D image stack is slow. Faster moving particles cannot be tracked.

To circumvent this problem, we realize that it is unnecessary to image a whole cell to follow the path of a single particle. We only have to take a snapshot of the particle and its immediate surroundings. If we know the origin of this snapshot and if we can determine the centroid of the particle, we can relocate the origin of the next snapshot to center the particle in the next image. This active feedback control reduces the size of the scan volume and the time required to scan this volume. The ultimate time resolution of this tracking system will depend on the electronic and the mechanical elements of this feedback loop which will be discussed in the following section. As a side note, this active feedback tracking system can also work with confocal detection but many added advantages of two-photon excitation, such as the reduction of sample photodamage, would be lost.

The active feedback tracking system can greatly increase the time resolution of but has one major limitation. In the presence of many small diffusing particles, the possibility of multiple particles entering into the excitation volume becomes appreciable. A smart feedback algorithm in the tracking system is critical and will help to alleviate this problem. Nevertheless, it is virtually impossible to guarantee against confusion when there is a high particle density. The only solution is to reduce the particle density such that the probability of having more than one particle in the volume of interest becomes negligible. However, this low particle density criterion creates a new problem. The interaction probability between a tracked particle and a particular cell becomes very low. One example is in the study of macrophage capture of antigenic particles and their subsequent phagocytosis. At very low antigen concentration, there is little chance that the antigenic particle being tracked will interact with a macrophage cell. A solution to this problem is to actively deliver the particle to the vicinity of the area under study, in this case, the cellular membrane surface. Therefore, the third major component of this instrument is an active particle delivery mechanism. Two methods will be considered. The most straightforward technique of using micropipettes for delivery has the advantage that particles as small as single proteins can be manipulated. A second, more elegant, technique which works with larger particles (0.5 to 10 microns) such as bacteria is the gradient optical trap (optical tweezers) (Ashkin, 1978; Svoboda and Block, 1994).

– *Applications*: One of the pilot application of two-photon single particle tracking involves the study of macrophage phagocytosis kinetics (So *et al.*, 1997). Although the general scheme of antigen capture and processing has been extensively stu-

died, kinetic studies *in vivo* are relatively rare. In this first study, the focus is on the capture of antigenic material, such as fluorescent *E. coli* bacteria or latex spheres, by murine macrophages. Using the gradient optical trap system, we were able to capture and transport 2 μm fluorescent latex spheres to a chosen macrophage cell. The spheres were positioned about 2 to 5 μm above the center of the cell. With the tracking circuit ready, the spheres were released and tracking began. Since the lateral dimension of the cell is large, on the order of 100 square microns, the possibility that diffusion would bring the proximally placed sphere to the cell surface is high. While most of the spheres drifted away, we have observed active capture of some spheres by the cell. A typical release and capture geometry of the spheres by the macrophage cell is shown in fig. 5. The track for the spheres that experienced some interaction but escaped is shown in fig. 6. The trajectory of a captured sphere is quite distinct (Fig. 7). After initial release of the sphere, some Brownian diffusion was observed. At a short time later, a rapid lateral translation is observed corresponding to a movement of 5 μm in less than 200 ms. Subsequent to the translation, the sphere is immobilized in the x-y plane within a diameter of 2 μm and within a axial position of 3 μm for the remainder of the experiment. After tracking, the sphere appears to be immobilized on the cell surface by visual inspection and the subsequent two-photon imaging generates fig. 5. This observation suggests that we have observed the kinetics of active capturing of antigenic material by a macrophage cell and that the capture speed is over 25 μm/s.

TIME SCALES: NANOSECONDS AND PICOSECONDS

Two-Photon Time-Resolve Microscopy

– *Significance*: In the nanosecond time scale, the application of fluorescence lifetime resolved techniques to fluorescence microscopy has opened up many exciting new opportunities. Lifetime-resolved imaging is a useful contrast enhancing mechanism. One of the common applications of fluorescence microscopy is to simultaneously image and distinguish various organelles in a single cell. Traditionally, these distinct cellular structures are labelled with specific fluorescent probes of sufficiently separated absorption spectra that each structure can be selectively excited by picking the proper excitation wavelength. By collecting a series of pictures with multiple excitation wavelengths, these pictures can be superimposed to generate an image in which the spatial relationship between these organelles is determined. This process not only requires multiple excitation light sources, achromatic optics and filter sets, but the sample must also be subjected to multiple exposures which may cause significant photodamage. This process can be greatly simplified by using lifetime resolved imaging. By labeling different organelles with dyes that have similar absorption spectra but different fluorescence lifetimes, these dyes can be excited and imaged with a single exposure and the organelles can be distinguished by their unique lifetime values. Under some circumstances, time-resolved imaging is simpler and more efficient than the traditional multiple-color labeling method. To characterize cellular micro-environments, it is often necessary to determine intracellular concentrations of biologically important substances such as Ca^{2+} and O_2 (Carrero *et al.*, 1992; Eberhard, and Erne, 1991; Grynkiewicz *et al.*, 1985; Minta *et al.*, 1989; Rink *et al.*, 1982). Fluorescence lifetime measurement is particularly useful with probes which changes their fluorescence intensity but not their spectra characteristics under different metabolite concentration such as Calcium Green or Flo3. In these cases, differential partitioning in cellular system prevents quantitative concentration determination. This problem of differential partitioning can be overcome with time-resolved techniques. The excited state lifetime is an intrinsic property of a fluorescence probe, and is independent of the probe concentration. The lifetime is sensitive to the probe's micro-environment, and the lifetime may change with the presence of certain chemical species. Specifically, there are fluorescent probes whose lifetime values are dependent upon the metabolite concentrations. For

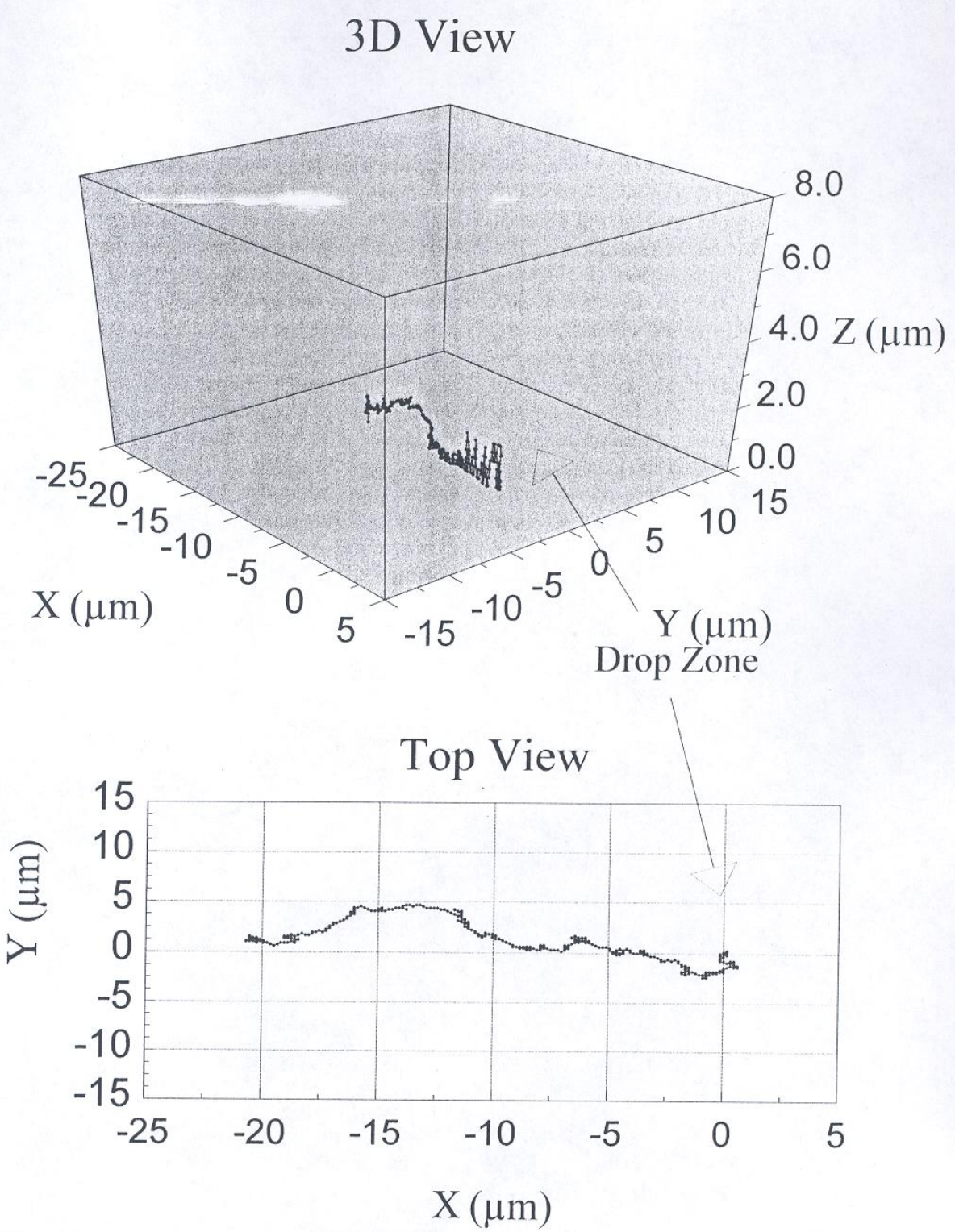

Fig. 6 *The trajectory of an escaped sphere.* The top panel is the 3D view and the bottom panel is the top view. Each time point in the trajectory is separated by 190 ms.

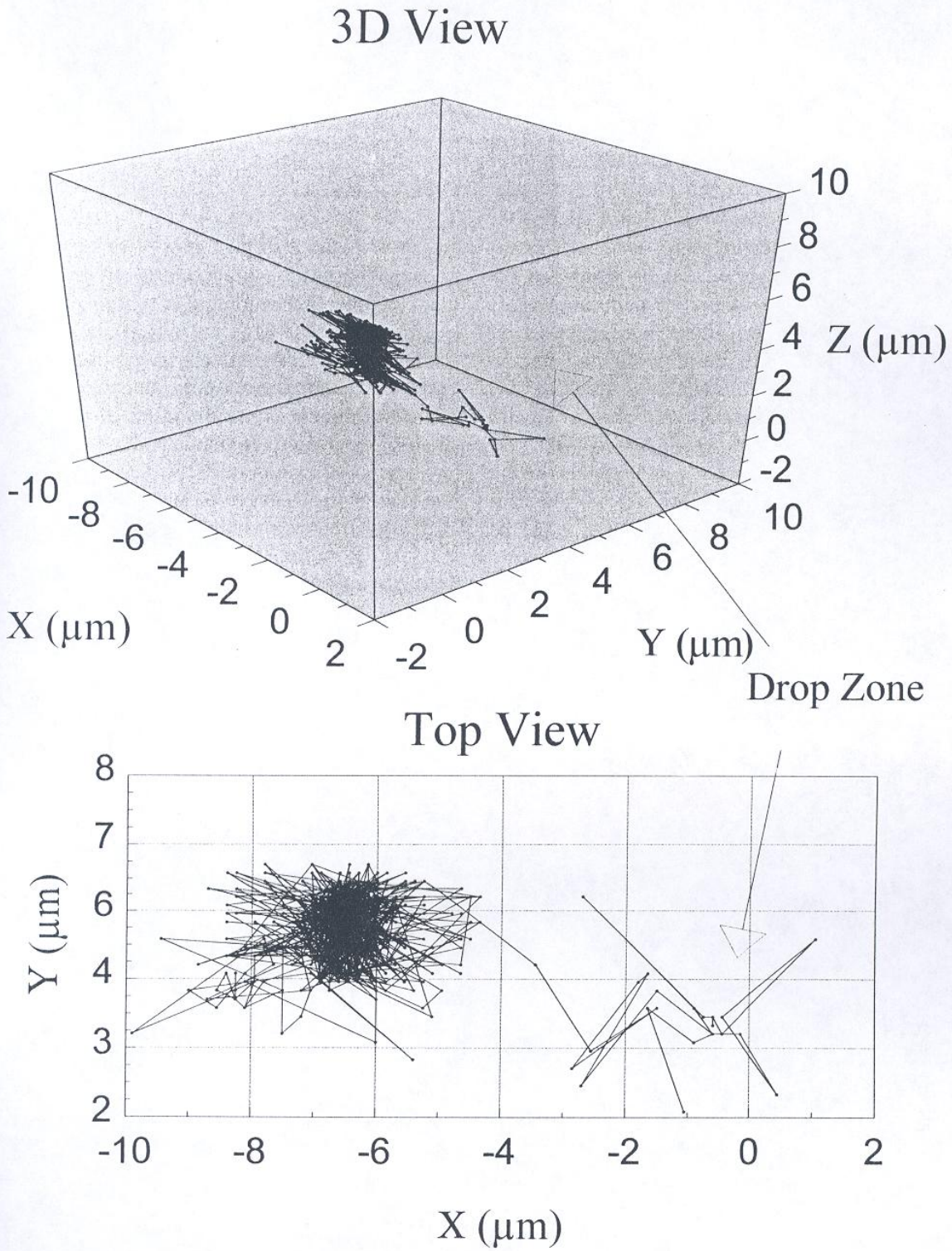

Fig. 7 *The trajectory of a captured sphere.* The top panel is the 3D view and the bottom panel is the top view. Each time point in the trajectory is separated by 190 ms.

example, intracellular calcium concentration has been determined from the lifetime measurement of Calcium Green and Crimson (Draaijer *et al.*, 1995; Sanders *et al.*, 1995; So *et al.*, 1995).

Frequency domain heterodyned time-resolved imaging.

– *Principles*: With one-photon excitation, lifetime resolved imaging has been performed using both frequency- and time-domain approaches. Although two-photon lifetime resolved imaging in the time domain remains to be attempted, the incorporation of two-photon microscopy with frequency domain lifetime resolved technique has been accomplished (French *et al.*, 1997; König *et al.*, 1996b; Masters *et al.*, 1997; So *et al.*, 1995). Time-resolved measurement in the frequency domain requires the use of intensity modulated light sources. In the simplest case, the light source is sinusoidally modulated. More complex excitation modulation is composed of multiple sinusoidal Fourier components. The fluorescence signal resulting from a sinusoidal excitation is also sinusoidal but it is phase delayed and de-modulated due to the finite lifetime of the chromophore (Fig. 8). The lifetime, τ, of a chromophore which exhibits a single exponential decay is simply related to its phase (ϕ) and modulation (M):

$$\tan(\phi) = \omega\tau$$

$$M = \frac{1}{\sqrt{1+\omega^2\tau^2}} \qquad (9)$$

where ω is the angular intensity modulation frequency. The task of lifetime measurement is reduced to the determination of the phase and modulation at an appropriate frequency. Since typical fluorescence lifetimes are on the order of nanoseconds, eq. 9 implies that the intensity modulation frequency should be on the order of tens to hundreds of mega-Hertz to obtain a phase shift and demodulation of measurable size. Accurate phase and modulation measurements at high frequency are difficult; however, high frequency phase and modulation information can be translated to a lower frequency carrier signal by heterodyning.

The heterodyning procedure involves the measurement of the fluorescence signal with a gain modulated detector. The detector gain modulation is at a

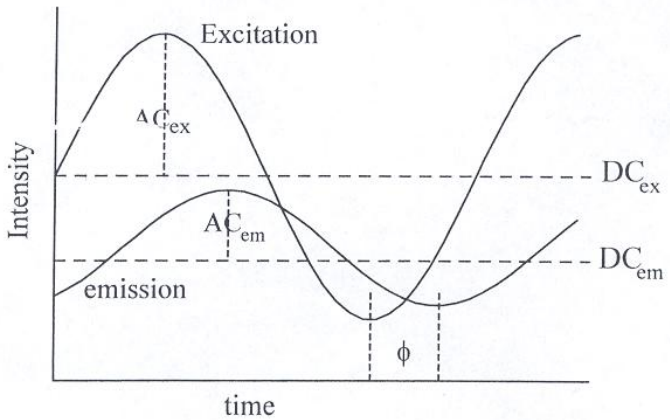

$$M = \frac{AC_{em}/DC_{em}}{AC_{ex}/DC_{ex}} \qquad \omega\tau = tan\phi \qquad \omega\tau = \sqrt{\frac{1}{M^2} - 1}$$

Fig. 8 *A measurement of fluorescence lifetime in the frequency domain involves the excitation of the fluorescence molecule using intensity modulated light.* Resulting from the finite lifetime of the chromophore, the emitted fluorescence will be phase delayed as well as demodulated (a decrease in the signal AC to DC ratio). The fluorescence lifetime can be deduced from the degree of phase delay and demodulation. In the case of single exponential decay, these simple relationships exist between these quantities.

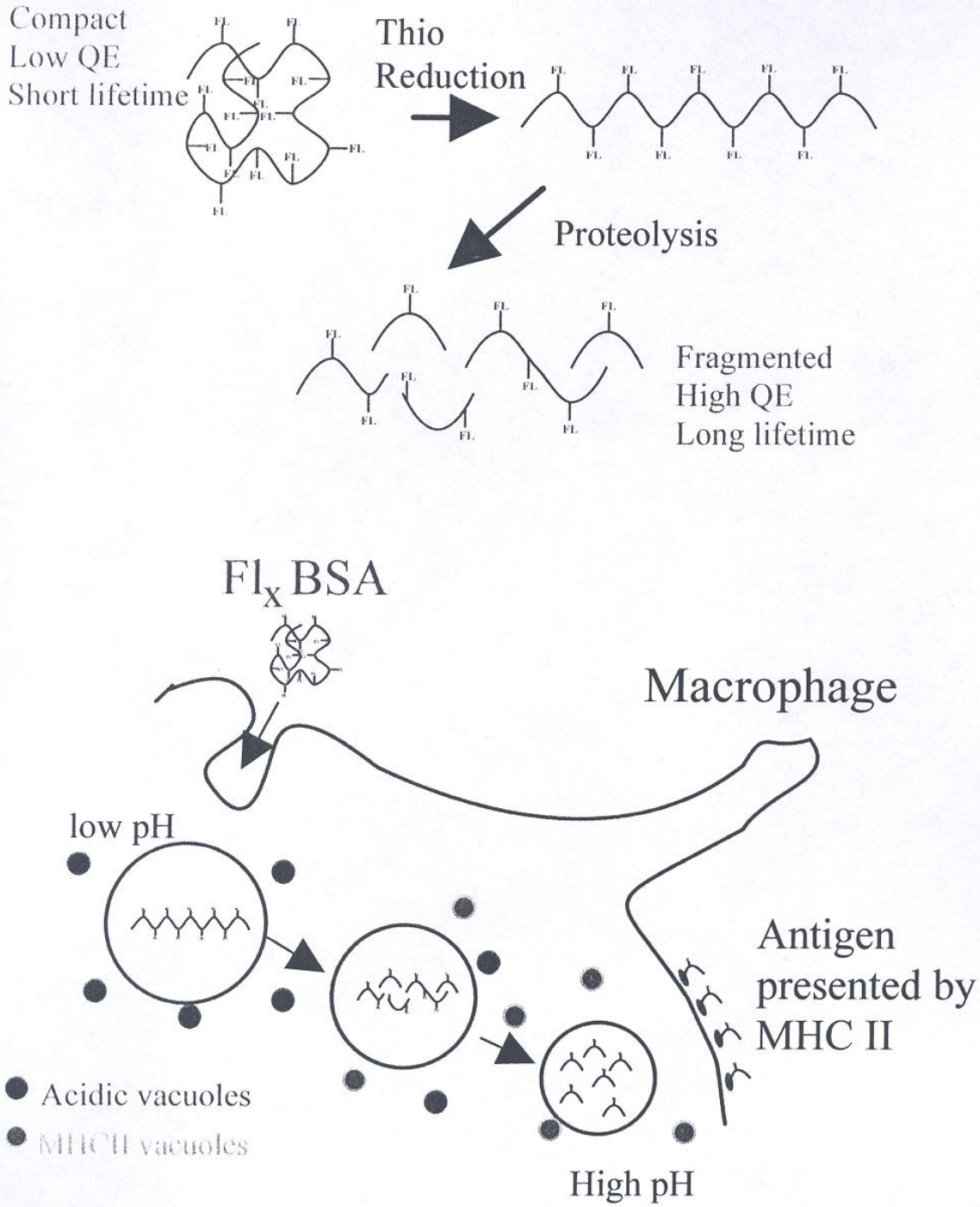

Fig. 9 *Biochemical basis for proteolysis measuring using the fluorescein-BSA probe.* The intact fluorescein-BSA has a low quantum yield and a short lifetime resulting from self quenching of the chromophores at a high conjugation ratio. Upon endocytosis, the proteolysis of these probes result in the fragmentation of the protein and increasing the mean distance between the fluorescein molecules. This fragmentation reduces self-quenching probability and the quantum yield. The lifetime of the fluorescein molecules increase. The degree of proteolysis of the antigen in the vacuoles can be correlated with the lifetime measured.

frequency ($\omega+d\omega$), equal to the excitation modulation frequency (ω) plus a small frequency difference ($d\omega$), the cross-correlation frequency. The detected light is modulated by the detector gain, and the two signals are mixed. Two new signals are generated at frequencies equal to the sum and the difference of the fluorescence modulation and the detector gain modulation. The frequency of the difference signal is the cross-correlation frequency, $d\omega$, and this low frequency signal retains the same phase and modulation information of the original fluorescence signal. Low pass filtering is used to isolate this low frequency signal from the other high frequency components. The cross-correlation signal is at sufficiently low frequency to be digitized, usually tens to hundreds of Hertz. The phase and modulation information can be extracted digitally via fast Fourier transform (FFT).

– *Applications*: As discussed, lifetime imaging can resolve multiple structures in cells and tissues similar to wavelength resolved imaging and it can also be used to quantitatively measure cellular metabolite concentration using non-ratiometric probes (So *et al.*, 1995). However, this technology excels in the study of cellular biochemical processes that has no wavelength sensitive probes. One important example is the monitoring of proteolysis processes (French *et al.*, 1997). An antigenic probe has been developed (Voss *et al.*, 1996). This probe is composed of fluorescein-bovine serum albumin (BSA) complexes. At a typical conjugation ratio from 15 to 22 fluorescein to one BSA, the complex has a very low fluorescence quantum yield as a result of self quenching between the fluorescein molecules. However, proteolysis of the protein results in the separation of the fluorescein moiety and the decrease in energy transfer between them. This reduces protein self quenching and significantly increases its quantum yield (Fig. 9). Furthermore, the fluorescein-BSA complex are able to trigger immunological response from macrophage cells and are internalized through either phagocytosis or endocytosis processes. Upon internalization, the complex are broken down through proteolysis processes inside the vacuoles of macrophages. Dramatic fluorescence intensity increase was observed upon the internalization of the complexes indicating proteolysis process have occurred. However, a quantitative measurement of proteolysis process is difficult since the concentration of the complexes in the vacuoles cannot be determined and the fluorescence intensity change do not provide quantitative information. On the other hand, it has been shown that the fluorescence lifetime of the fluorescein moiety in the fluorescein-BSA complex is sensitive to the protein environment. The lifetime of fluorescein is below 500 ps but increases to the normal fluorescein lifetime of 4 ns upon proteolysis of the complex. Therefore, a lifetime map can provide a quantitative measurement of the degree of proteolysis (Fig. 10).

Another important example is the use of fluorescence lifetime to measure the cellular and tissue redox state. Redox state was measured by monitoring cellular auto-fluorescence lifetime from endogenous chromophores which primarily consist of β-nicotinamide-adenine dinucleotide phosphate (NAD(P)H). NAD has a fluorescence decay time of about 400 ps. Bound NAD(P)H has a blue shifted emission spectrum and a lifetime of 2 ns. Typically, a higher metabolic rate generates a higher concentration of NAD(P)H and produces an image with longer lifetime. This technique has been used to monitor cellular redox state changes upon photostress (König *et al.*, 1996) and to access cellular activity of *in vivo* human epidermal tissue (Masters *et al.*, 1997). For example, this lifetime technique has been used to successfully confirm NAD(P)H as the

page 789

Fig. 10 *Fluorescence intensity and lifetime images of mouse macrophage cells after internalizing fluorescein-BSA complexes.* Note that the two large vacuoles on the left side of the cell (arrow) show significant intensity difference. It would be erroneous to conclude that the vacuoles are at a different stages of proteolysis as the lifetime picture indicate that both vacuoles have the same lifetime. The result is consistent with these two vacuoles have a different quantity of fluorescein-BSA content.

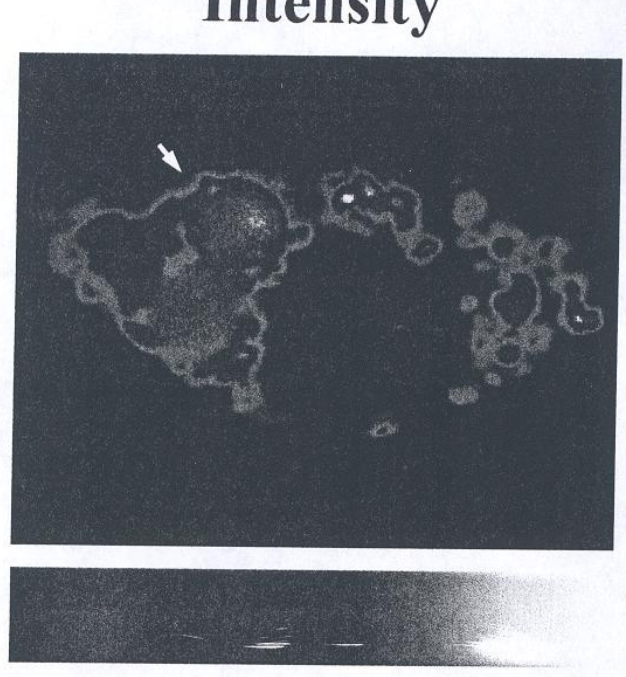
Intensity
0
1000
(A.U.)
Lifetime
0
4.5
(ns)

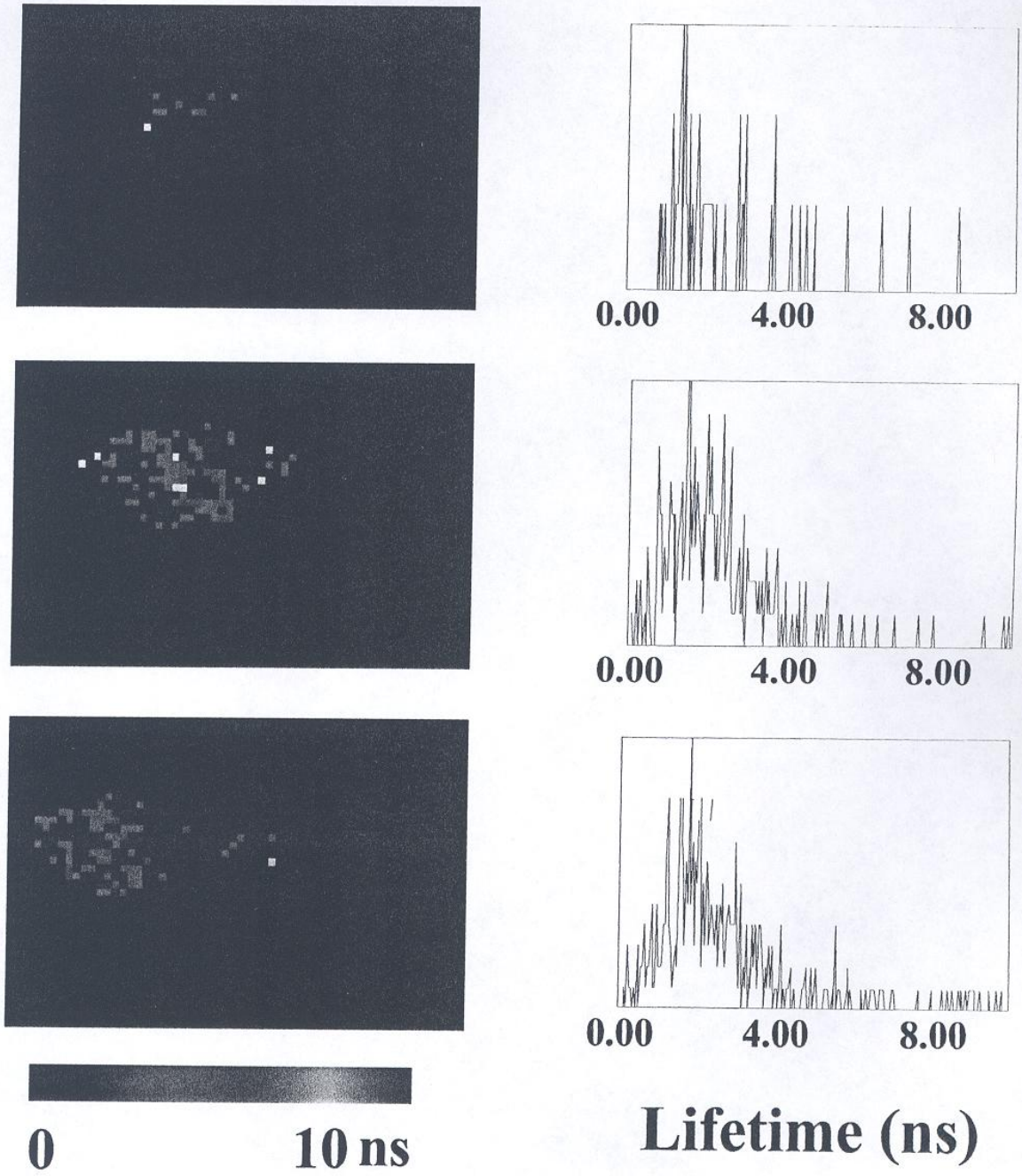

Fig. 11 *NAD(P)H is the most probably source of autofluorescence of a photodamaged sperm.* The lifetime of the sperm autofluorescence has a mean of 2 ns which is consistent with NAD(P)H fluorescence. Time-resolved images of the sperm under successive scan are shown on the left and the lifetime distributions of all the valid pixels in the images are shown on the right.

major source of the autofluorescence observed during the photodamage of human sperm (Fig. 11).

CONCLUSION

A decade after the invention of two-photon microscopy, the utility of this technique in obtaining three dimensional spatial resolved information from living systems has been well demonstrated. The future development of this technique involves the incorporation of spectroscopic information to extract biological functional data. The minimally invasive nature of two-photon microscopy makes it the ideal technique to observe the evolution of living biological system over time. Today, the combinations of a variety of time-resolved methodologies with two-photon microscopy have yielded a number of new techniques. Many of these techniques are at the beginning stage of their development. However, given the promising results shown in their pilot studies, these new time-resolve two-photon microscopy techniques may provides unique information that can further our understanding in many areas of biology and medicine.

REFERENCES

Ashkin, A., Trapping of atoms by resonance radiation pressure. *Phys. Rev. Lett.* 1978, **40**: 729-732.

Bailey, B., Farkas, D.L., Taylor, D.L. and Lanni, F., Enhancement of axial resolution in fluorescence microscopy by standing-wave excitation. *Nature* 1993, **366**: 44-48.

Berland, K.M., So, P.T.C., Chen, Y., Mantulin, W.W. and Gratton, E., Scanning two-photon fluctuation correlation spectroscopy: particle counting measurements for detection of molecular aggregation. *Biophys. J.* 1996, **71**: 410-420.

Berland, K.M., So, P.T.C. and Gratton, E., Two-photon fluorescence spectroscopy: method and application to the intracellular environment. *Biophys. J.* 1995, **68**: 694-701.

Bhawalkar, J.D., Shih, A., Pan, S.J., Liou, W.S., Swiatkiewicz, J., Reinhardt, B.A., Prasad, P.N. and Cheng, P.C., Two-photon laser scanning fluorescence microscopy – from a fluorphore and specimen perspective. *Bioimaging* 1996, **4**: 168-178.

Carrero, J., French, T. and Gratton, E., Oxygen imaging in tissues. *Biophys. J.* 1992, **59**: 167a.

Cheong, W.F., Prahl, S.A. and Welch, A.J., A review of the optical properties of biological tissues. *IEEE J. Quantum Electr.* 1990, **26**: 2166-2185.

Cohen, C.J., Bacon, R., Clarke, M., Joiner, K. and Mellman, I., Dictyostelium discoideum mutants with conditional defects in phagocytosis. *J. Cell Biol.* 1994, **126**: 955-966.

Cunningham, M.L., Johnson, J.S., Giovanazzi, S.M. and Peak, M.J., Photosensitized production of superoxide anion by monochromatic (290-405 nm) ultraviolet irradiation of NADH and NADPH coenzymes. *Photochem. Photobiol.* 1985, **42**: 125-128.

Denk, W., Two-photon scanning photochemical microscopy: Mapping ligand-gated ion channel distributions. *Proc. natn. Acad. Sci.* USA 1994, **91**: 6629-6633.

Denk, W., Strickler, J.H. and Webb, W.W., Two-photon laser scanning fluorescence microscopy. *Science* 1990, **248**: 73-76.

Deurs, B.V., Petersen, O.W., Olsnes, S. and Sandvig, K., The way of endocytosis. *Int. Rev. Cytol.* 1989, **117**: 131-177.

Dingwall, C. and Laskey, R., The nuclear membrane. *Science* 1992, **258**: 942-947.

Draaijer, A., Sanders, R. and Gerritsen, H.C., Fluorescence lifetime imaging, a new tool in confocal microscopy, In: *Handbook of biological Confocal Microscopy*, Pawley, J.B. (ed.). Plenum Press, New York, 1995, pp. 491-505.

Eberhard, M. and Erne, P., Calcium binding to fluorescent calcium indicators: Calcium Green, Calcium Orange and Calcium Crimson. *Biochem. biophys. Res. Commun.* 1991, **180**: 209-215.

Elson, E.L. and Magde, D., Fluorescence correlation spectroscopy. I. Conceptual basis and theory. *Biopolymers* 1974, **13**: 1-27.

Elson, E.L., Magde, D. and Webb, W.W., Fluorescence correlation spectroscopy. II. An experimental realization. *Biopolymers* 1974, **13**: 29-61.

Fahey, P.F. and Webb, W.W., Lateral diffusion in phospholipid bilayer membranes and multilamellar liquid crystal. *Biochemistry* 1978, **17**: 3046-3054.

Fein, M., Unkeless, J., Chuang, F.Y.S., Sassaroli, M., Costa, R.D., Vaananen, H. and Eisinger, J., Lateral mobility of lipid analogues and GPI-anchored proteins in supported bilayers determined by fluorescent bead tracking. *J. Memb. Biol.* 1993, **133**: 83-92.

French, T., So, P.T.C., Carrero, J., Weaver, D.J.Jr., Cherukuri, A., Zoelho-Sampaio, T., Gratton, E. and Voss, E., Macrophage mediated processing of an exogenous probe: elucidation of probe processing with two-photon fluorescence microscope with time-resolved and intensity imaging. *J. Microsc.* 1997, **185**: 339-353.

Ghosh, R.N. and Webb, W.W., Results of automated tracking of low density lipoprotein receptors on cell surfaces. *Biophys. J.* 1988, **53**: 352a.

Ghosh, R.N. and Webb, W.W., Automated detection and tracking of individual and clustered cell surface low density lipoprotein receptor molecules. *Biophys. J.* 1994, **66**: 1301-1318.

Goldstein, J.L., Brown, M.S., Anderson, R.G.W., Russell, D.W. and Schneider, W.J., Receptor-mediated endocytosis: concepts emerging from the LDL receptor system. *Ann. Rev. Cell Biol.* 1985, **1**: 1-39.

Göppert-Mayer, M., Über Elementarakte mit zwei Quantensprungen. *Ann. Phys.* Leipzig 1931, **5**: 273-294.

Grynkiewicz, G., Poenie, M. and Tsien, R.Y., A new generation of Ca^{2+} indicators with greatly improved fluorescence properties. *J. biol. Chem.* 1985, **260**: 3440-3450.

Haugland, R.P., *Handbook of Fluorescence Probes and Research Chemicals*. Molecular Probes, Oregan, 1997.

Hell, S.W., Lindek, S. and Stelzer, E.H.K., Enhancing the axial resolution in far-field light microscopy: two-photon excitation 4Pi-confocal fluorescence microscopy. *J. Mod. Opt.* 1994, **41**: 675-681.

Hell, S. and Stelzer, E.H.K., Fundamental improvement of resolution with a 4Pi-confocal fluorescence microscope using two-photon excitation. *Opt. Commun.* 1992, **93**: 277-282.

Hicks, B.W. and Angelides, K.J., Tracking movement of lipids and Thy 1 molecules in the plasmalemma of living fibroblasts by fluorescence video microscopy with nanometer scale precision. *J. Memb. Biol.* 1995, **144**: 231-244.

Huang, Y.C. and Graves, D.J., Correlation between subunit interactions and enzymatic activity of phosphorylase a. Method for determining equilibrium constant from initial rate measurement. *Biophys. J.* 1970, **70**: 2001-2007.

Igarashi, H, Takahashi, E., Hiroi, M. and Doi, K, Aging-related changes in calcium oscillations in fertilized mouse oocytes. *Mol. Reprod. Dev.* 1997, **48**: 383-390.

Jacobson, K., Sheets, E.D. and Simson, R., Revisiting the fluid mosaic model of membranes. *Science* 1995, **268**: 1441-1442.

Kao, H.P. and Verkman, A.S., Tracking of single fluorescent particles in three dimensions: use of cylindrical optics to encode particle position. *Biophys. J.* 1994, **67**: 1291-1300.

Kinjo, M. and Rigler, R., Ultrasensitive hybridization analysis using fluorescence correlation spectroscopy. *Nucl. Acid Res.* 1995, **23**: 1795-1799.

Kirby, M.S., Hadley, R.W. and Lederer, W.J., Measurement of intracellular Ca^{2+} concentration using Indo-1 during simultaneous flash photolysis to release Ca^{2+} from DM-nitrophen. *Pflugers Arch.* 1994, **427**: 169-177.

König, K., Krasieva, T., Bauer, E., Fiedler, U., Berns, M.W., Tromberg, B.J. and Greulich, K.O., Cell damage by UVA radiation of a mercury microscopy lamp probed by autofluorescence modification, cloning assay and comet assay. *J. Biomed. Opt.* 1996a, **1**: 217-222.

König, K., So, P.T.C., Mantulin, W.W. and Gratton, E., Cell damage in two-photon femtosecond microscopes. *Appl.Opt.* 1997, **22**: 135.

König, K., So, P.T.C., Mantulin, W.W., Tromberg, B.J. and Gratton, E., Two-photon excited lifetime imaging of autofluorescence in cells during UVA and NIR photostress. *J. Micros.* 1996b, **183**: 197-204.

Krawczyk, W.S., A pattern of epidermal cell migration during wound healing. *J. Cell Biol.* 1971, **49**: 247-263.

Lipp, P., Kleinle, J., Amstutz, C., Luscher, C. and Niggli, E., Two-photon point photolysis of caged Ca^{2+}. *Biophys. J.* 1997, **72**: A44.

Luby-Phelps, K., Taylor, D.L. and Lanni, R., Probing the structure of cytoplasm. *J. Cell Biol.* 1986, **102**: 2015-2022.

Maniak, M., Rauchenberger, R., Albrecht, R., Murphy, J. and Gerisch, G., Coronin involved phagocytosis: dynamics of particle-induced relocalization visualized by a green fluorescent protein tag. *Cell* 1995, **83**: 915-924.

Masters, B., So, P.T.C. and Gratton, E., Multiphoton excitation fluorescence microscopy and spectroscopy of *in vivo* human skin. *Biophys. J.* 1997, **72**: 2405-2412.

Masters, B.R. and Thaer, A.A., Real-time scanning slit confocal microscopy of the *in vivo* human cornea. *Appl. Opt.* 1994, **33**: 695-701.

McCray, J.A. and Trentham, D.R., Properties and uses of photoreactive caged compounds. *Annu. Rev. Biophys. Biophys. Chem.* 1989, **18**: 239-270.

Mertz, J., Xu, C. and Webb, W.W., Single molecule detection by two-photon excited fluorescence. *Opt. Lett.* 1995, **20**: 2532-2534.

Meyer, T. and Schindler, H., Particle counting by fluorescence correlation spectroscopy: simultaneous measurement of aggregation and diffusion of molecules in solution and in membranes. *Biophys. J.* 1988, **54**: 983-993.

Minta, A., Kao, J.P.Y. and Tsien, R.Y., Fluorescent indicators for cytosolic calcium based on rhodamine and fluorescein chromophores. *J. biol. Chem.* 1989, **264**: 8171-8178.

Morisaki, J.H., Heuser, J.E. and Sibbley, L.D., Invasion of *Toxoplasma gondii* occur by active penetration of the host cell. *J. Cell Sci.* 1995, **108**: 2457-2464.

Niggli, E. and Lederer, W.J., Molecular operations of the sodium-calcium exchanger revealed by conformation currents. *Nature* 1991, **349**: 621-624.

Oehlenschlager, F., Schwille, P. and Eigen, M., Detection of HIV-1 RNA by nucleic acid sequence based amplification combined with fluorescence correlation spectroscopy. *Proc. natn. Acad. Sci.* USA 1996, **93**: 12811-12816.

Oh, Y.K. and Straubinger, R.M., Intracellular fate of *Mycobacterium avium*: Use of dual-label spectrofluorometry to investigate the influence of bacterial viability and opsonization on phagosomal pH and phagosome-lysosome interaction. *Infect. Immun.* 1996, **64**: 319-325.

Oneill, R.E., Jaskunas, R., Blobel, G., Palese, P. and Moroianu, J., Nuclear import of influenze virus RNA can be mediated by viral nucleoprotein and transport factors required for protein import. *J. biol. Chem.* 1995, **270**: 22701-22704.

Palecek, S.P., Loftus, J.C., Ginsberg, M.H., Lauffenburger, D.A. and Horwitz, A.F., Integrin-ligand binding properties govern cell migration speed through cell-substratum adhesiveness. *Nature* 1997, **385**: 537-540.

Palmer, A.G. and Thompson, N.L., Molecular aggregation characterized by high order auto-correlation in fluorescence correlation spectroscopy. *Biophys. J.* 1987, **52**: 257-270.

Palmer, A.G. and Thompson, N.L., Intensity dependence of high order autocorrelation functions in fluorescence correlation spectroscopy. *Rev. Sci. Instr.* 1989, **60**: 624-633.

Piston, D.W., Masters, B.R. and Webb, W.W., Three-dimensionally resolved NAD(P)H cellular metabolic redox

imaging of the *in situ* cornea with two-photon excitation laser scanning microscopy. *J. Micros.* 1995, **178**: 20-27.

Rauer, B., Neumann, E., Widengren, J. and Rigler, R., Fluorescence correlation spectrometry of the interaction kinetics of tetramethylrhodamine alpha-bungarotoxin with Torpedo Californica acetylcholine receptor. *Biophys. Chem.* 1996, **58**: 3-12.

Rink, T.J., Tsien, R.Y. and Pozzan, T., Cytoplasmic pH and free Mg^{2+} in lymphocytes. *J. Cell Biol.* 1982, **95**: 189-196.

Rothman, J.E., Mechanism of intracellular protein transport. *Nature* 1994, **372**: 55-63.

Ruan, K. and Weber, G., Physical heterogeneity of muscle glycogen phosphorylase revealed by hydrostatic pressure dissociation. *Biochemistry* 1993, **32**: 6295-6301.

Salmeen, I., Zacmanidis, P., Jesion, G. and Feldkamp, L.A., Motion of mitochondria in cultured cells quantified by analysis of digitized images. *Biophys. J.* 1985, **48**: 681-686.

Sanders, R., Draaijer, A., Gerritsen, H.C., Houpt, P.M. and Levine, Y.K., Quantitative pH imaging in cells using confocal fluorescence lifetime imaging microscopy. *Anal. Biochem.* 1995, **227**: 302-308.

Sandvig, K., Gerred, O., Prydz, K., Kolov, J.V., Hansen, S.H. and Deurs, B.V., Retrograde transport of endocytosed Shiga toxin to the endoplasmic reticulum. *Nature* 1992, **358**: 510-512.

Santana, L.F., Kranias, E.G. and Lederer, W.J., Calcium sparks and excitation-contraction coupling in phospholamban-deficient mouse ventricular myocytes. *J. Physiol.* London 1997, **503**: 21-29.

Saxton, M.J., Single-particle tracking: models of directed transport. *Biophys. J.* 1994, **67**: 2110-2119.

Schmidt, C.E., Chen, T. and Lauffenburger, D.A., Simulation of integrin-cytoskeletal interaction in migrating fibroblasts. *Biophys. J.* 1994, **67**: 461-474.

Schwartz, A., Cell biology of intracellular protein trafficking. *Annu. Rev. Immunol.* 1990, **8**: 195-229.

Sheetz, M.P., Turney, S., Qian, H. and Elson, E.L., Nanometer-level analysis demonstrates that lipid flow does not drive membrane glycoprotein movement. *Nature* London 1989, **340**: 284-288.

Sheppard, C.J.R. and Gu, M., Image formation in two-photon fluorescence microscopy. *Optik* 1990, **86**: 104-106.

Sheppard, C.J.R. and Gu, M., Image formation in two-photon fluorescence microscopy. *Optik* 1992, **92**: 102.

Shore, J.D. and Chakrabarti, S.K., Subunit dissociation of mitochondrial malate dehydrogenase. *Biochemistry* 1976, **15**: 875-879.

Stenn, K.S. and DePalma, L., Re-epithelialization. In: *The molecular and cellular Biology of Wound Repair* (1st ed.), Clark, R.A.F. and Henson, P.M. (eds.), Plenum Press, New York, 1988, Chapter 14.

So, P.T.C., French, T., Yu, W., Berland, K.M., Dong, C.Y. and Gratton, E., Time-resolved fluorescence microscopy using two-photon excitation. *Bioimaging* 1995, **3**: 49-63.

So, P.T.C., Ragan, T., Gratton, E., Carrero, J. and Voss, E., Two-photon single particle tracking in 3D. *SPIE Proc.* 1997, **2983**: 45-56.

Svoboda, K. and Block, S.M., Biological applications of optical forces. *Annu. Rev. Biophys. Biomol. Struct.* 1994, **23**: 247-285.

Voss, E.W.Jr., Workman, C.J. and Mummert, M.E., Detection of protease activity using a fluorescence-enhancement globular substrate. *BioTechn.* 1996, **20**: 286-291.

Watts, C. and Marsh, M., Endocytosis: what goes in and how? *J. Cell Sci.* 1992, **103**: 1-8.

White, J.G., Amos, W.B. and Fordham, M., An evaluation of confocal verse conventional imaging of biological structures by fluorescence light microscopy. *J. Cell Biol.* 1987, **105**: 41-48.

Widengren, J., Mets, U. and Rigler, R., Fluorescence correlation spectroscopy of triplet state in solution – a theoretical and experimental study. *J. Chem. Phys.* 1995, **99**: 13368-13379.

Wilson, T., Confocal microscopy. In: *Confocal Microscopy*, Wilson, T. (ed.), Acad. Press, London. 1990, pp. 1-60.

Wokosin, D.L., Centonze, V.E., Crittenden, S. and White, J.G., Three-photon excitation fluorescence imaging of biological specimens using an all-solid-state-laser. *Bioimaging* 1996b, **4**: 208-214.

Wokosin, D.L., Centonze, V., White, J.G., Armstrong, D., Roberson, G. and Ferguson, A.I., All-solid-state ultrafast lasers facilitate multiphoton excitation fluorescence imaging. *IEEE J. sel. Top. Quantum Electr.* 1996a, **2**: 1051-1065.

Xu, C., Shear, J.B. and Webb, W.W., Hyper-rayleigh and hyper-Raman scattering background of liquid water in two-photon excited fluorescence detection. *Anal. Chem.* 1997, **69**: 1285-1287.

Xu, C., Zipfel, W., Shear, J.B., Williams, R.M. and Webb, W.W., Multiphoton fluorescence excitation: New spectral windows for biological nonlinear microscopy. *PNAS* USA 1996, **93**: 10763-10768.